

showing peptic activity on the gel, designated as band I to band VI, with decreasing anodal mobilities. In the case of adult forestomach, band III shows the strongest activity, followed by bands IV and I, while band VI is very faint. When pH of the crude extract of the adult forestomach was brought to 2.0 with HCl prior to the electrophoresis, all bands showed increased mobility towards the anodal end, suggesting that the materials in the bands were pepsinogens, and they gave rise to corresponding pepsins by activation.

The zymogram pattern of the crude extract of forestomach of 15-day or 20-day embryos differed from that of the adult. Band I was completely absent in 15-day extract (figure 2, a), band II being the major one. In the extract from the 20-day embryonic forestomach (figure 2, b), band I appeared in some cases, but in small quantity. Band II almost disappeared, and bands V and VI became prominent. The activity of band III was very weak in the embryonic forestomach. The disappearance of band II in the later embryonic period suggests that the material in band II is specific for the young embryonic forestomach.

After hatching, the zymogram pattern changed rapidly to the adult type, together with the rise in total peptic activity. Thus, 36 and 60 h after hatching (figure 2, d and e), the zymogram pattern was almost identical to that of the adult, though that of the 12-h chick (figure 2, c) resembled the embryonic pattern.

The possible relationship between feeding, and the change in peptic activity after hatching, was compared by the zymogram patterns of fed and unfed chicks. The zymogram patterns were completely identical between the 2 groups.

Though differences in electrophoretic mobility do not necessarily mean qualitatively different proteins, and would also include conformational changes and differences in charge, our study indicated that band I differs immunologically from the other bands<sup>5</sup>.

The rapid increase of the activity and changes of molecular species of digestive enzymes at the time of hatching were observed also for maltase in the chick jejunum<sup>8</sup>. It was

suggested that these changes are regulated by hormones, especially by hydrocortisone, as hydrocortisone has an enhancing effect on the level of digestive enzymes *in vivo*<sup>8</sup> and *in vitro*<sup>9,10</sup>. In the rat stomach, the maturation of the chief cells, the increase in peptic activity and the change of molecular species of pepsinogens occur at the time of weaning<sup>11</sup>, and these events are also regulated by hydrocortisone<sup>12,13</sup>, suggesting that similar mechanisms are involved in the control of the digestive enzymes around the time of hatching in birds and the time of weaning in mammals. The avian pepsinogens might be a useful probe for the study of these regulatory mechanisms because of the rapid change at the time of hatching and the ease of its purification<sup>5</sup>.

- 1 We thank Dr A. Glucksmann, Cambridge, for reading the manuscript and helpful discussion, and Dr T. Sugimura, National Cancer Center, Tokyo, for his interest in our work. This work was supported by Grants-in-Aid for Cancer Research from the Ministry of Education, Science and Culture, Japan, and by Grant from the Toray Science Foundation.
- 2 T. Mizuno and S. Yasugi, *C.r. Acad. Sci., Serie D* 276, 1609 (1973).
- 3 S. Yasugi and T. Mizuno, *Wilhelm Roux Arch.* 174, 107 (1974).
- 4 S. Yasugi, *C.r. Acad. Sci., Serie D* 283, 179 (1976).
- 5 H. Esumi, S. Yasugi, T. Mizuno and H. Fujiki, *Biochim. biophys. Acta*, submitted.
- 6 S. T. Donta and H. Van Vunakis, *Biochemistry* 9, 2791 (1970).
- 7 S. Yasugi, Thesis, University of Tokyo 1976.
- 8 J. Dautlick, Jr, and C. F. Strittmatter, *Biochim. biophys. Acta* 222, 447 (1970).
- 9 J. C. Hijmans and K. S. McCarty, *Proc. Soc. exp. Biol. Med.* 123, 633 (1966).
- 10 B. L. Black and F. Moog, *Dev. Biol.* 66, 232 (1978).
- 11 C. Furihata, Y. Iwasaki, T. Sugimura, M. Tatematsu and M. Takahashi, *Cell Different.* 2, 179 (1973).
- 12 C. Furihata, T. Kawachi and T. Sugimura, *Biochem. biophys. Res. Commun.* 47, 705 (1972).
- 13 M. Kumegawa, T. Takuma, S. Hosoda, S. Kunii and Y. Kanda, *Biochim. biophys. Acta* 543, 243 (1978).

## Density gradient centrifugation of cells separated from multicellular tumor spheroids<sup>1</sup>

C. P. Sigdestad<sup>2</sup>, D. J. Grdina and K. Ando

*Section of Experimental Radiotherapy, University of Texas System Cancer Center, M. D. Anderson Hospital & Tumor Institute, 6723 Bertner Avenue, Houston (Texas 77030, USA), 20 September 1978*

**Summary.** Cells from a murine fibrosarcoma (FSA) have been grown *in vitro* as multicell tumor spheroids (MTS). The growth rate of these MTS was determined. Following selected periods of growth, MTS were made into a single cell suspension and separated on linear density gradients of Renografin. While only 1 population of cells was separated from small spheroids (400  $\mu\text{m}$  diameter), at least 3 subpopulations of tumor cells were separated and isolated from large spheroids (800  $\mu\text{m}$  in diameter).

Multicellular tumor spheroids (MTS) have been used successfully as an *in vitro* model of tumor growth<sup>3</sup>. MTS retain inherent advantages of cell culture such as simplicity, low cost, and environmental control while exhibiting cell-to-cell contact<sup>4</sup>, chronically hypoxic cell populations<sup>5</sup> and gompertzian growth patterns<sup>6</sup>. Grdina et al.<sup>7</sup> have shown that density gradient centrifugation of cells separated from a solid tumor isolates multiple bands of cells which show biophysical as well as physiological differences. Density separation of exponentially growing CHO cells show only 1 density band while starved late stationary cultures have at

least 3 density populations<sup>8</sup>. These changes suggest the influence of cell environment on the banding patterns obtained. The purpose of the present study was to determine density banding patterns in MTS during growth.

**Materials and methods.** A methylcholanthrene induced murine fibrosarcoma (FSA) in C3H mice was used throughout this study. In each experiment 4-6 tumors were dissected and made into single cells by the method previously described by Grdina et al.<sup>9</sup>. MTS were grown using the soft agar method described by Macpherson<sup>10</sup>. Briefly, approximately  $10^6$  FSA cells in 10 ml of Eagle's Basal

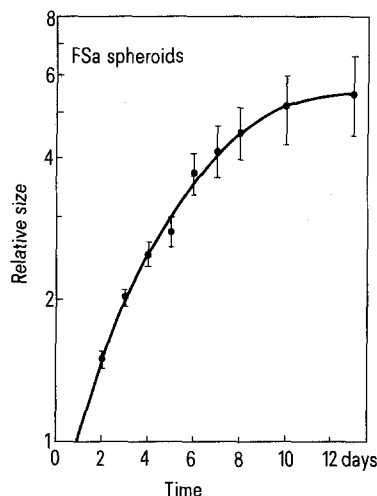


Fig. 1. Relative growth rate of fibrosarcoma (FSa) tumor cells grown as multicellular tumor spheroids (MTS).

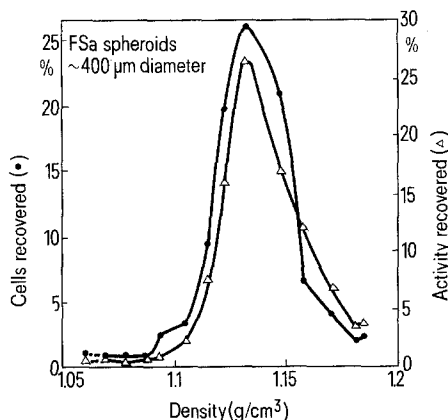


Fig. 2. Density gradient centrifugation of FSa tumor cells separated from MTS of 400  $\mu\text{m}$  diameter (after 2 days growth). Circles (●) represent total cell recovery while triangles ( $\Delta$ ) represent  $^3\text{HTdR}$  labeled cell recovery per density increment.

Medium (EBM) were plated in stationary 100-mm plastic Petri dishes that had a 2–3-mm base layer of 0.5% Nobel agar in EBM. The MTS were allowed to grow at 37°C in a water saturated atmosphere of 5%  $\text{CO}_2$  and 95% air.

The growth rate of MTS was measured by transferring individual spheroids into 16-mm wells (Co-star No.3524) treated as described above. The MTS were sized daily with a calibrated reticle in an inverted microscope. Spheroid size relative to the day of transplanting was plotted against time.

The density banding experiments were performed at 2 and 8 days after plating. MTS of similar sizes (approximate diameter of 400 and 800  $\mu\text{m}$  respectively) were labeled with tritiated thymidine ( $^3\text{HTdR}$ , 0.5  $\mu\text{Ci}/\text{ml}$ ) for 30 min, then cold thymidine was added to prevent further uptake of label. The MTS were dissociated with 0.25% trypsin, the cells counted and viability (94%) determined by phase contrast microscopy. Approximately  $10^7$  cells were layered on 14 ml preformed gradients (10–35% Renografin in Ringers solution), centrifuged at  $13,000 \times g$  for 30 min in a swinging bucket rotor (Beckman L5-50, SW27.1 rotor) at 4°C. The entire gradient was fractionated into 1-ml samples. The refractive index ( $N_{24}$ ) was determined for each fraction and the density calculated using the formula p

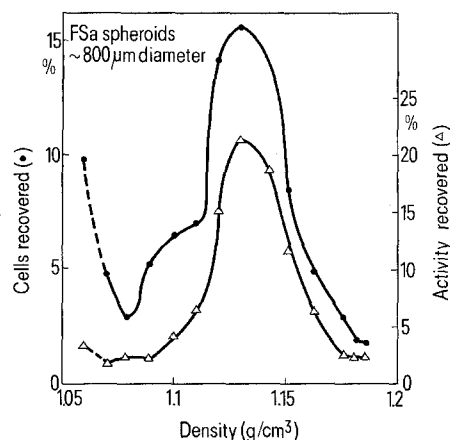


Fig. 3. Density gradient centrifugation of FSa tumor cells separated from MTS of 800  $\mu\text{m}$  diameter after 8 days growth. Circles (●) represent total cell recovery while triangles ( $\Delta$ ) represent  $^3\text{HTdR}$  labeled cell recovery per density increment.

( $\text{g}/\text{cm}^3$ ) =  $3.4683 \times N_{24} 3.6267$ . The number of cells was determined using a hemacytometer and phase contrast microscope. The  $^3\text{HTdR}$  uptake was determined using the method described by Meistrich et al.<sup>11</sup>. This involved pipetting a known number of cells on GF/C glass fibre filter paper, washing twice each with cold phosphate buffered saline, 5% cold trichloroacetic acid and 95% ethanol. The filter paper was air-dried in liquid scintillation vials; 1 ml of NCS solubalizer was added and the vials were allowed to stand overnight at room temperature. 10 ml of scintillation cocktail were added and the samples counted in a liquid scintillation counter. The data was presented as per cent total cells and per cent total activity recovered per density increment.

**Results and Discussion.** The growth curve for fibrosarcoma tumor cells grown as multicellular spheroids is presented in figure 1. The growth was exponential for the first 7 days when the curve began to bend into a Gompertzian type function. The doubling time was about 3 days during early MTS growth. The results were similar to those reported by Yuh<sup>12</sup>.

Isopycnic banding of FSa tumor cells derived from MTS with an approximate diameter 400  $\mu\text{m}$  (after 2 days growth) are presented in figure 2. Only a single band of cells was observed at a density of 1.13  $\text{g}/\text{cm}^3$ . There is a slight but perhaps significant indication of a band forming at 1.10  $\text{g}/\text{cm}^3$ . The  $^3\text{HTdR}$  activity follows the cell recovery curve indicating that under the conditions tested, the isolated cell population is comprised mainly of proliferative cells.

Figure 3 presents data obtained from cells isolated from spheroids with a diameter of about 800  $\mu\text{m}$  (after 8 days growth). Under these conditions 3 bands of cells are noted at 1.06, 1.11, and 1.13  $\text{g}/\text{cm}^3$ , respectively. The latter band is identical to the one noted in small MTS. It appears that 2 less dense bands of cells were formed as the MTS doubled in size. The  $^3\text{HTdR}$  activity recovered follows only the band formed at 1.13  $\text{g}/\text{cm}^3$  which indicates the less dense cells may be out of the proliferative cell cycle.

Durand<sup>13</sup> utilized velocity sedimentation in isolating cell subpopulations from exponential and plateau phase cells as well as multicellular spheroids. Ng and Inch<sup>14</sup> using Ficoll gradients found a single density band in EMT6 tumor cells isolated from spheroids. We confirm these findings in small spheroids but find 2 additional less dense bands appear when spheroids are allowed to grow and reach diameters of 800  $\mu\text{m}$  or more.

- 1 This investigation was supported in part by grants numbered CA-18628 and CA-06294, awarded by the National Cancer Institute, DHEW.
- 2 On leave of absence from: Department of Therapeutic Radiology, University of Louisville, 500 S. Floyd St., Louisville, Kentucky 40202, USA.
- 3 R.M. Sutherland and R.E. Durand, *Curr. Top. Radiat. Res. Quart.* **11**, 87 (1976).
- 4 R.E. Durand and R.M. Sutherland, *Exptl Cell Res.* **71**, 75 (1972).
- 5 R.M. Sutherland, J.A. McCredie and W.R. Inch, *J. natl Cancer Inst.* **46**, 113 (1971).
- 6 A.C. Burton, *Growth* **30**, 157 (1966).
- 7 D.J. Grdina, I. Basic, K.A. Mason and H.R. Withers, *Radiat. Res.* **63**, 483 (1975).
- 8 D.J. Grdina, M.L. Meistrich and H.R. Withers, *Exptl Cell Res.* **85**, 15 (1974).
- 9 D.J. Grdina, L. Milas, K.A. Mason and H.R. Withers, *J. natl Cancer Inst.* **52**, 253 (1974).
- 10 L. Macpherson, in: *Methods and Applications*, p.276. Ed. P.F. Kruse and M.K. Patterson. Academic Press, London and New York 1973.
- 11 M.L. Meistrich, *J. Cell Physiol.* **80**, 299 (1972).
- 12 J.M. Yuhas, *Cancer Res.* **37**, 3639 (1977).
- 13 R.E. Durand, *Cancer Res.* **36**, 1295 (1975).
- 14 C.E. Ng and W.R. Inch, *J. natl Cancer Inst.* **60**, 1017 (1978).

### A note on the mechanism of action of UV-irradiation of amphibian embryos

C.J. Duncan

*Department of Zoology, University of Liverpool, P.O. Box 147, Liverpool L69 3BX (England), 2 October 1978*

**Summary.** The actions on amphibian embryos of UV-irradiation, exposure to  $\text{Li}^+$  or exposure to ouabain show interesting parallels with their effects on spontaneous release at the presynaptic terminals of the neuromuscular junction. It is suggested that these treatments serve to raise intracellular  $\text{Ca}^{2+}$  ( $[\text{Ca}^{2+}]_i$ ) in these examples, and that UV-promoted abnormalities in embryogenesis are a consequence of changes in  $[\text{Ca}^{2+}]_i$  at critical stages in development.

Two treatments that are known to produce abnormal development in amphibian embryos are exposure to UV-irradiation or to salines containing high concentrations of  $\text{Li}^+$ .

$\text{Li}^+$  has a typical 'vegetalising' action and produces characteristic abnormalities in which the normal balance of cell populations and the control of morphogenesis are disturbed<sup>1</sup>.  $\text{Li}^+$  presumably accumulates intracellularly and is not readily removed by the cation pump<sup>2</sup>. The way in which  $\text{Li}^+$  produces these effects is unknown, but biochemical comparisons between experimental and control embryos have shown several differences at the transcriptional and translational level<sup>1</sup> and it is suggested that the delay in cell differentiation of ectoderm is related to a lesion in the mechanisms of gene expression<sup>3</sup>.  $\text{Li}^+$  has also been implicated in modifying cAMP levels via its inhibitory action on adenylate cyclase<sup>4</sup>. It may decrease the rate of cell division<sup>5</sup> and it has been suggested that it causes sub-lethal cytotoxicity<sup>6</sup>. We have now shown that intracellular accumulation of  $\text{Na}^+$ , produced by treating *Xenopus* embryos with ouabain, the inhibitor of the cation pump, also causes abnormal development<sup>2</sup>.

UV-irradiation of the vegetal hemisphere leads to abnormalities in neural morphogenesis<sup>7</sup> and also to a complete subsequent absence of primordial germ cells, although primordial germ cells can be re-established if vegetal pole cytoplasm is injected into the vegetal hemisphere of irradiated eggs<sup>8-10</sup>. This action of UV-irradiation on the primordial germ cells has been of particular interest to embryologists; it has been suggested that the target for UV-irradiation is nucleic acid<sup>8</sup> or nucleoprotein<sup>11</sup>. The initial effect of UV-irradiation is an inhibition of cleavage, although nuclear division continues so that a syncytium is formed<sup>11,12</sup>. This inhibition of cytokinesis by UV-irradiation has also been shown in sea urchin eggs, cultured mammalian cells, protozoans and *Drosophila* eggs (see Beal and Dixon<sup>11</sup>).

There is an interesting parallel with the effects of these treatments on the rate of spontaneous release of transmitter at the amphibian neuromuscular junction, as measured by the frequency of the miniature endplate potentials

(MEPPs). Exposure to  $\text{Li}^+$  saline<sup>13-15</sup>, or treatment with ouabain<sup>16-18</sup> or UV-irradiation<sup>19</sup> all produce a marked rise in MEPP frequency. There is good evidence that MEPP frequency is determined primarily by  $[\text{Ca}^{2+}]_i$  at the presynaptic terminals<sup>20</sup>. Thus,  $\text{Li}^+$ -saline and ouabain both promote a rise in intracellular alkali metal cations which, in turn, causes a rise in  $[\text{Ca}^{2+}]_i$ <sup>21,22</sup> probably by release of  $\text{Ca}^{2+}$  from storage sites; both  $\text{Na}^+$  and  $\text{Li}^+$  have been shown to cause a dramatic release of  $\text{Ca}^{2+}$  from isolated mitochondria<sup>23,24</sup>. UV-irradiation at 255 nm (a wavelength close to that used in many of the studies with amphibian embryos) has been shown to act at a protein site essential for  $\text{Ca}^{2+}$ -binding on the inner face of crab axon<sup>25</sup>. It is concluded that these treatments all serve to increase MEPP frequency by raising  $[\text{Ca}^{2+}]_i$  at the presynaptic terminals.

UV-irradiation of sea urchin eggs extends the time of the increased  $\text{Ca}^{2+}$ -ATPase activity during the 1st part of the cell cycle if the eggs are irradiated before fertilization. Irradiation at 50 min after fertilization causes delay of the 2nd cell cycle and also extends the increased  $\text{Ca}^{2+}$ -ATPase activity of the 1st part of the 2nd cycle. The  $\text{Ca}^{2+}$ -ATPase itself, however, is not directly sensitive to UV-irradiation<sup>26</sup>.

It is therefore suggested that  $\text{Li}^+$ -saline<sup>2</sup> and UV-irradiation could both produce abnormalities in amphibian development by causing, initially, a rise in  $[\text{Ca}^{2+}]_i$  in the embryos. Thus, the level of  $[\text{Ca}^{2+}]_i$  produces a graded control of junctional permeability in *Chironomus* salivary gland cells, thereby providing a means of selective transmission of intercellular molecular signals<sup>27</sup>. Such an explanation would be in accord with recent studies with the divalent cation ionophore A23187 which suggest that an experimentally-induced rise in  $[\text{Ca}^{2+}]_i$  in *Xenopus* embryos interferes with normal, integrated cell division<sup>2</sup>.

- 1 M. Stanisstreet and J. Osborn, *Life Sci.* **18**, 451 (1976).
- 2 J.C. Osborn, C.J. Duncan and J.L. Smith, *J. Cell Biol.* **80**, 589 (1979).
- 3 J.L. Smith, J.C. Osborn and M. Stanisstreet, *J. Embryol. exp. Morph.* **36**, 513 (1976).
- 4 D. McMahon, *Science* **185**, 1012 (1974).